A&A 395, 233–242 (2002)
DOI: 10.1051/0004-6361:20021280
© ESO 2002

Astronomy & Astrophysics

The abundance of gaseous H_2O and O_2 in cores of dense interstellar clouds

H. Roberts[1] and E. Herbst[2]

[1] Department of Physics, The Ohio State University, Columbus, OH 43210, USA
[2] Departments of Physics and Astronomy, The Ohio State University, Columbus, OH 43210, USA

Received 21 May 2002 / Accepted 30 August 2002

Abstract. We have used chemical models that include both gas-phase and grain-surface processes to try to understand the low water and molecular oxygen abundances inferred from SWAS observations towards dense molecular clouds. The models represent an improvement over pure gas-phase chemistries in that they are more realistic, and they are largely successful at reproducing the low O_2 abundances. For cold clouds, such as TMC-1 and L134N, the limits on the H_2O abundance are met by the models only after relatively long periods of accretion (10^6–10^7 yr), but we show that ground-based observations of these clouds do not necessarily contradict these ages, especially for L134N. If the upper limits on the H_2O abundance were to be revised downwards, however, or if water were to be observed in the cold clouds at the same level as in some star-forming regions, then even heavier depletions would be required. For this reason, the low H_2O abundance observed by SWAS in ρ Oph cannot be reproduced by the models without calculating unphysically low abundances of CO.

Key words. ISM: abundances – ISM: molecules – molecular processes

1. Introduction

The primary goals of the "Submillimeter Wave Astronomical Satellite" (SWAS; Melnick et al. 2000) were to observe the abundance and distribution of gas-phase oxygen and carbon in the interstellar medium (ISM). The chemical composition of interstellar clouds is important in studies of ionisation fraction and chemical balance. These observations set out to confirm long standing predictions of gas-phase chemical models that H_2O and O_2 are major reservoirs of atomic oxygen in cold, dense clouds and are important coolants of the gas.

Gas-phase chemical models of quiescent cloud cores typically predict steady-state molecular oxygen abundances of $\sim 10^{-5}$ and water abundances of a few times 10^{-7}, relative to H_2 (Bergin et al. 1996; Lee et al. 1996a; Millar et al. 1997). Results from SWAS, however, indicate that these species are actually far less abundant. Goldsmith et al. (2000) searched for O_2 in 20 sources, but made no convincing detections. The limits on O_2 abundance they determined were $<3 \times 10^{-6}$ in TMC-1 and L134N, and $<10^{-7}$ towards most other sources. A recent tentative detection of O_2 at a fractional abundance of 10^{-5} has been made (Goldsmith et al. 2001), but the source is a molecular outflow towards ρ Oph A rather than a dense core. Snell et al. (2000b) detected H_2O towards several star-forming regions, with abundances of only 6×10^{-10}–10^{-8}, and did not detect water in the dark clouds TMC-1, L134N, and B335, with the strongest upper limit being $<7 \times 10^{-8}$.

The above observations impose a new set of constraints on interstellar chemical models. Bergin et al. (2000) discussed some explanations for the low oxygen and water abundances in dense cores. The simplest explanation is chemical youth, but although this is reasonable for molecular oxygen, a species that takes a long time to reach steady state, it is less reasonable for water, which reaches too large an abundance too quickly. One can assume that the branching fraction for production of H_2O in the dissociative recombination of H_3O^+ is very low (Williams et al. 1996), but this result is in disagreement with other recent experiments (Vejby-Christensen et al. 1997; Neau et al. 2000; Jensen et al. 2000). Bergin et al. (2000) also considered models with a high C/O elemental abundance ratio and more dynamic gas-grain models in which O and C atoms accrete onto surfaces and form water and methane, respectively. The methane is released back into the gas phase, enhancing the carbon chemistry but the water remains on the grains. Finally, Bergin et al. mentioned other possibilities such as shocks, turbulence, and cycling of material between low- and high-density phases, the latter two mechanisms serving to maintain an apparent chemical youthfulness. The role of shocks has been studied to a greater degree by Charnley et al. (2001). The role of accretion has been explored by Viti et al. (2001), who considered cyclic gas-phase models in which CO and N_2 are allowed to accrete onto grains and return to the gas-phase when other heavy molecules remain on the grains. They also suggested that the high ionisation

Send offprint requests to: E. Herbst,
e-mail: herbst@mps.ohio-state.edu

Article published by EDP Sciences and available at http://www.aanda.org or http://dx.doi.org/10.1051/0004-6361:20021280

phase of bistable models provides a natural explanation for the low abundance of oxygen.

Another explanation of the low water and oxygen abundances is based on the low spatial resolution of SWAS. The SWAS beam can be as large as 4 arcmin. Unless the morphology of the region is completely determined, the observed abundances cannot be deconvoluted and may represent averages over areas with differences in physical conditions and/or significant gradients in molecular abundances. Spaans & van Dishoeck (2001) have constructed models of clumpy molecular clouds, both with and without nearby stars. For quiescent sources as well as sources near young stars, they find a significant decrease in the average abundances of oxygen and water compared with homogeneous models. The effect is mainly due to photodissociation. Their agreement with the SWAS results is reasonable for S140 but less so for ρ Ophiuchi. Photodissociation also plays a large role in the explanation provided by Casu et al. (2001) who emphasize that dust coagulation can reduce the far-UV extinction of dust grains sufficiently that photodissociation removes gas-phase water and molecular oxygen rapidly.

The constraints on chemical models of dense cores become more stringent when combined with recent observations of interstellar ices. The Infrared Space Observatory (ISO) found water ice to be abundant in dense clouds, with a fractional abundance of $\sim 10^{-4}$ with respect to H_2. CO_2 is also an abundant ice component towards both active star forming regions and quiescent clouds. Gerakines et al. (1999) found its abundance to be typically 10–20% of water ice, while Nummelin et al. (2001) found CO_2/H_2O to be up to 0.37 in the ices towards some sources. On the other hand, Vandenbussche et al. (1999) searched for O_2 ice towards cold, dense clouds, obtaining only an upper limit of $O_2/H_2O < 0.2$ towards NGC 7538 IRS9.

We have recently developed models of gas-grain chemistry in cold cloud cores which simultaneously follow the chemistry that occurs in the gas and on grain surfaces in some detail (Ruffle & Herbst 2000, 2001a, 2001b). The model has previously been used mainly to understand observations of interstellar ices, but its predictions for gas-phase species are also germane. Despite the fact that desorption, induced by cosmic ray bombardment, is included, results strongly depart from pure gas-phase models at times greater than 10^5 yr. Indeed, there is a strong interaction between surface chemistry and desorption. It seems reasonable to apply this model to the problem posed by the SWAS observations, especially those objects for which the model was designed – cold, dark clouds. We also use the gas-grain model to study chemical abundances in some warmer regions, also observed by SWAS, to probe the expected water and oxygen abundances in such sources.

2. The models

The gas-grain models are those described in Ruffle & Herbst (2000, 2001a; hereafter RHI and RHII), in which gas-phase and grain surface chemistries are linked through accretion and desorption processes. These models were developed in response to new experimental data on the surface mobility of hydrogen atoms on olivine and amorphous carbon (Katz et al. 1999) and so incorporate slower rates of diffusion of species across grain surfaces than was previously assumed. The kinetic equations used for surface diffusion are taken from the modified rate equation approach of Caselli et al. (1998) and Shalabiea et al. (1998), although the need for modifications is greatly reduced owing to the low diffusion rates employed (see RHI). We are using the versions of the models which incorporate surface photochemistry (RHII).

There are two sets of gas-grain models. In the first case, atomic H is the only species with reduced mobility relative to that used in previous models, and the diffusion of H is not fully slowed to the extent measured by Katz et al. (1999), since that would mean it moves more slowly than other, heavier, species. In the second case, therefore, where H *is* slowed to the measured rate, the diffusion rates of all other species are slowed proportionally. In the discussion which follows, models where only H atoms are slowed are referred to as P1 (for an olivine surface) and P1/ac (for amorphous carbon). Models P2 and P2/ac represent models on olivine and amorphous carbon surfaces, respectively, where all diffusion rates have been slowed.

Although it is becoming increasingly clear that simple gas-phase chemistries are unrealistic even in quiescent clouds, they have been used in the past. Therefore, for completeness, we also present some results from a pure gas-phase chemistry, where the only surface reaction included is for the formation of H_2 (Bettens et al. 1995; Lee et al. 1996a).

Throughout, the grains are assumed to have radii of 0.1 μm and 10^6 binding sites. These canonical values (Tielens & Allamandola 1987) represent the peak of the grain size distribution; in future models we hope to consider both smaller and larger grains as well. The cosmic ray ionisation rate is $1.3 \times 10^{-17}\,s^{-1}$. Unless otherwise stated, gas-phase species other than hydrogen (H_2) are initially atomic with the "low-metal" abundances listed in RHI and Lee et al. (1996a).

3. Cold clouds

Dark, quiescent clouds, such as TMC-1 and L134N, have temperatures $\sim$10 K and H_2 densities of $\sim 10^4$ cm^{-3} (Pratap et al. 1997; Dickens et al. 2000). Figure 1 shows the evolution of selected gas-phase abundances from gas-grain models under these conditions. Only grain-surface chemistry on olivine is considered here, since experiments show that diffusion on amorphous carbon occurs so slowly at 10 K that the chemistry will not proceed. As well as H_2O and O_2, we have plotted the abundances of CO, NH_3 and HC_3N over time, since one of the observational constraints is that the low H_2O and O_2 abundances inferred by SWAS are towards regions where significant abundances of other molecules *are* present. Carbon monoxide is included as the most abundant interstellar molecule (after H_2) and provides some measure of the overall depletion, while cyanoacetylene (HC_3N) is included as a representative of organic molecules.

The major differences between models P1 and P2 occur at times $>10^7$ yr. The slow diffusion rates for all species in model P2 mean that grain surface chemistry occurs slowly and there are more small species on the grain surfaces which desorb more easily. Overall, therefore, freeze-out is not so

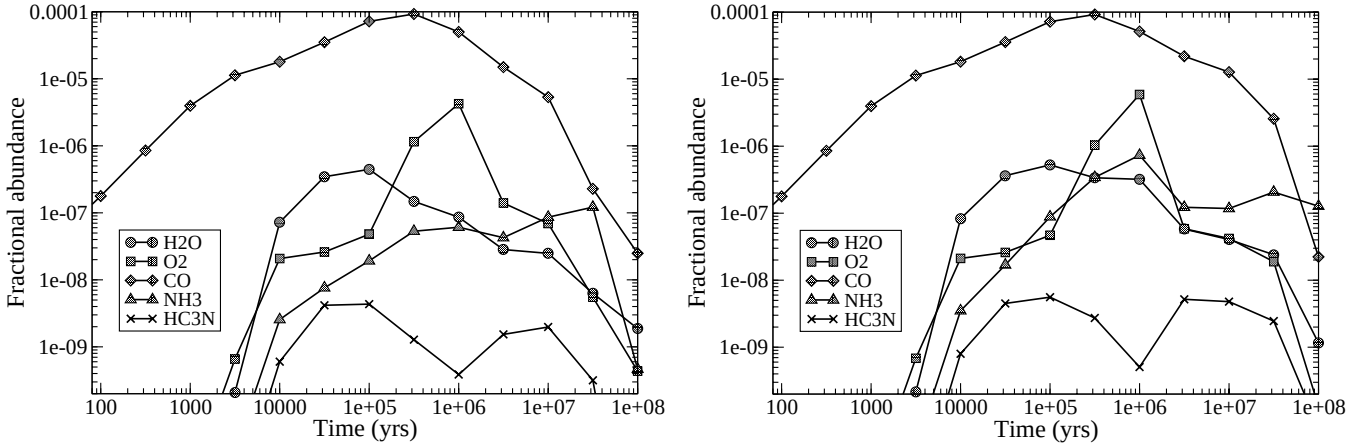

Fig. 1. Predicted gas-phase molecular abundances vs. time, from models P1 (left) and P2 (right). $T = 10$ K; $n(H_2) = 10^4$ cm^{-3}.

efficient at late times. Even though both accretion and desorption mechanisms act in these models, a steady-state chemistry is not reached. The abundances of many gas-phase species, including CO, H_2O and O_2, rise until somewhere between 10^5 and 10^6 yr, at which time freeze-out begins to dominate and their abundances decline. With such behaviour, molecules such as O_2, that take a significantly long time to reach a high abundance in gas-phase models, are never able to reach this abundance in gas-grain models. A closer look at the temporal dependence of the O_2 abundance shows a peak that lasts a relatively short time.

Let us look in somewhat more detail at the processes governing the abundances of gas-phase water and molecular oxygen. Water is formed in the gas phase mainly through a sequence of reactions starting with that between atomic oxygen and the ion H_3^+ and ending with the dissociative recombination of the ion H_3O^+. Meanwhile, a far larger amount of water is formed on grain surfaces via hydrogenation of O atoms by H atoms. Molecular oxygen is formed in the gas phase via a variety of neutral-neutral reactions (e.g. O + OH) and on the surfaces of grains via recombination between surface O atoms. Once accreted onto dust grains, water is inefficiently desorbed in our models via both cosmic ray desorption and thermal evaporation (Fraser et al. 2001). Surface molecular oxygen is desorbed at about the same slow rate as CO via cosmic rays (Hasegawa & Herbst 1993) and is actually depleted more rapidly by reactions in model P1, so that even less returns to the gas than in model P2.

The increase in gaseous abundance followed by a decrease when accretion becomes important is not universal. The NH_3 abundance, for example, remains relatively high (10^{-7} with respect to H_2) until 3×10^7 yr in model P1 and at least 10^8 yr in model P2, while for HC_3N the accretion actually causes a secondary "late-time" abundance peak of $(2–5) \times 10^{-9}$ after $\sim 10^7$ yr. This result, which holds for all cyanopolyynes, was first noted by Ruffle et al. (1997).

Looking specifically at water and molecular oxygen, we see that H_2O falls below the limits set by SWAS towards cold clouds for times $>10^6$ yr, at which times the O_2 abundances are also well below the observed upper limits. A simple explanation of the SWAS results, therefore, lies in adopting time scales somewhat larger than usually considered in gas-phase models.

The timescale for accretion in gas-grain models is largely dependent on the density, which governs the number of collisions between gas-phase molecules and grains, and on the so-called "sticking coefficient", the probability that a molecule colliding with a grain will freeze onto it. In the models discussed here, we have adopted a sticking coefficient of 0.5, but we have investigated the effects of varying its value between 0.1 and 1. For times up to a few times 10^5 yrs, the results are the same. At later times, the higher the sticking coefficient, the more rapidly the gas-phase species freeze out and the less pronounced the secondary peak in the cyanopolyyne abundances. However, for times $<10^7$ yr, varying the sticking coefficient does not change the abundances of the species discussed here by more than an order of magnitude.

In the following sections we compare our model results with observations of the sources TMC-1 and L134N, which have previously been studied in some detail by ground-based telescopes, and investigate whether the timescales necessary to reproduce the SWAS results are reasonable.

3.1. TMC-1

In order to illustrate that the limits on H_2O and O_2 abundance set by SWAS were surprisingly low, Fig. 2 shows how the predicted abundances from a pure gas-phase chemistry (the so-called new standard model; see Terzieva & Herbst 1998) match observations of the "cyanopolyyne peak" in TMC-1 as a function of time. The comparison for H_2O, O_2, and CO is plotted explicitly, while other species are considered together. As noted by previous authors (Terzieva & Herbst 1998; Bettens et al. 1995), best agreement for most species is at "early time" ($\sim 10^5$ yr). Here, almost 80% of the abundances observed by Ohishi et al. (1992) and Ohishi & Kaifu (1998) are matched by the gas-phase model to within an order of magnitude. However, although the O_2 abundance is well below the upper limit set by SWAS, the water abundance is at least ten times too high. Once steady state is reached, the overall agreement has dropped to $\sim$20%, and both O_2 and H_2O abundances are 7–8 times higher than the observational limits.

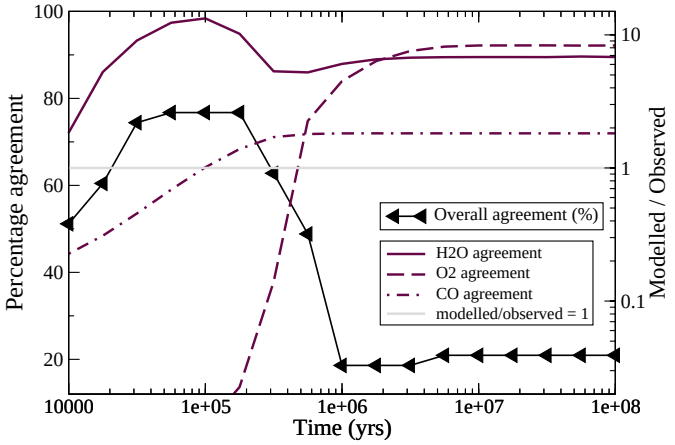

Fig. 2. The left-hand axis and solid line with triangles represent the percentage agreement for 43 species, to within a factor of 10, between a pure gas-phase chemistry (T = 10 K, $n(H_2) = 10^4$ cm^{-3}) and the TMC-1 observations of Ohishi et al. (1992) and Ohishi & Kaifu (1998). The right-hand axis and the solid, dashed and dash-dotted lines represent the ratios of the predicted abundances of H_2O, O_2 and CO, respectively, to the limits set/observed abundances towards TMC-1.

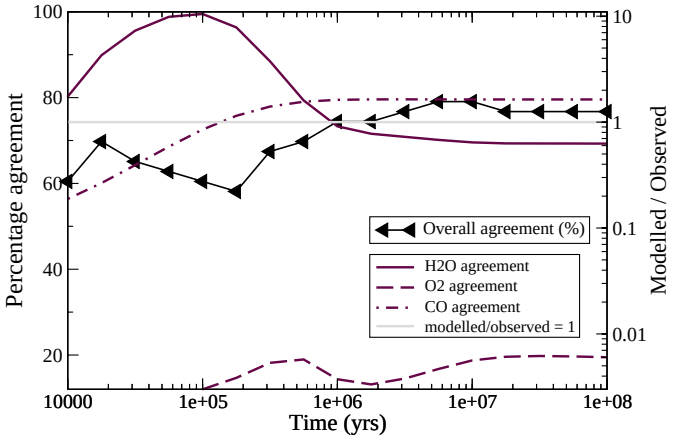

Fig. 3. As in Fig. 2, but from a gas-phase model using a C/O elemental ratio of 1.

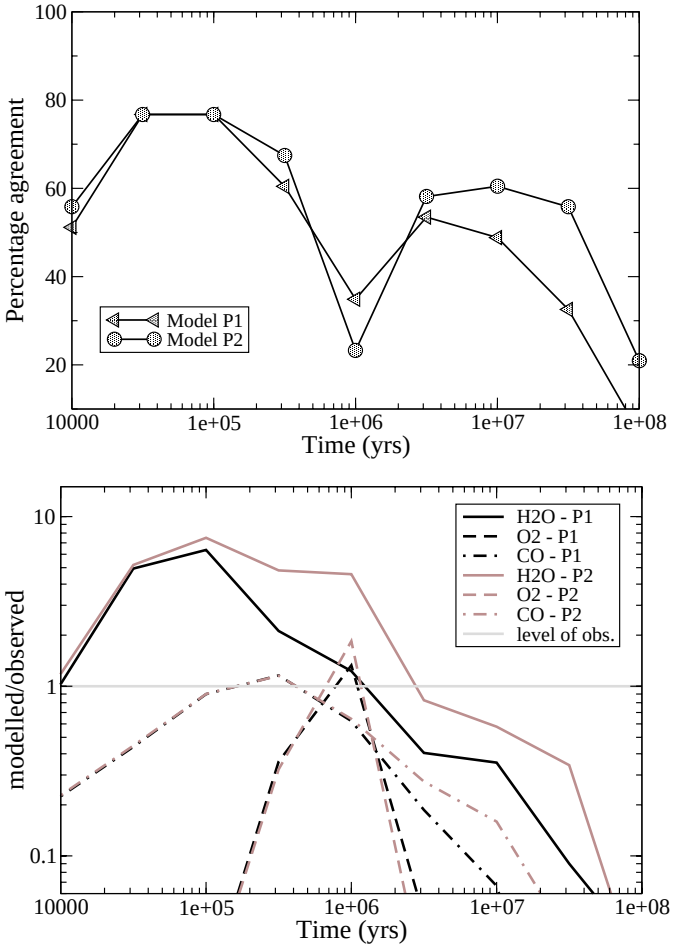

Fig. 4. Top: The percentage agreement of a gas-grain chemistry (T = 10 K, $n(H_2) = 10^4$ cm^{-3}) with the observations of Ohishi et al. (1992) and Ohishi & Kaifu (1998). BOTTOM: The ratios of the predicted abundances of H_2O, O_2 and CO to the limits set/observations made towards TMC-1.

Bergin et al. (2000) found that an increase in the elemental C/O ratio from the solar value of 0.4 to >0.9 allows H_2O and O_2 abundances to agree with the SWAS observations at later, more relevant times. Terzieva & Herbst (1998) showed that varying the C/O ratio in their gas-phase model affects the agreement with observations of TMC-1. In particular, they found that the time of best agreement tends to increase with increasing C/O ratio, but presented no specific predictions for H_2O and O_2.

Figure 3, therefore, shows the agreement over time for the gas-phase model in which elemental oxygen has been depleted so that C/O = 1. Again, the agreement for H_2O, O_2 and CO is plotted explicitly, while the percentage agreement is given for the less abundant species. The time of best agreement (nearing the 80% level) is now between 5×10^6 and 10^7 yr, when O_2 and CO are also in good agreement with the observations, and the H_2O abundance has dropped slightly below the SWAS limit.

Experimental evidence does suggest that H_2O is more tightly bound to grains than CO, and this might provide some explanation as to why there should be a differential depletion between carbon and oxygen. Nevertheless, a more realistic treatment should provide some reason for depletions as a function of time. Earlier models of TMC-1 (e.g. Ruffle et al. 1997; Markwick et al. 2000; Hartquist et al. 2001) have included accretion onto and desorption from grain surfaces. Our gas-grain model does provide a detailed description for differential depletion rates through cosmic ray desorption (Hasegawa & Herbst 1993), which yields varying desorption rates for individual species based on the strength of their attachment to grain particles. The physics of this mechanism for desorption is, however, treated only in an approximate fashion, and the desorption rates may not be sufficiently accurate for our purposes.

RH1 note that the overall level of agreement between the gas-grain models with initial low-metal gas-phase abundances and the abundances of the gas-phase molecules detected in TMC-1 does not decrease monotonically from the early-time peak, as occurs in the oxygen-rich gas-phase model, but shows a second peak of considerable agreement between a few times 10^6 and 10^7 yr. This is illustrated in the top panel of Fig. 4, for gas-grain models P1 and P2. Model P2 is in

Table 1. A comparison of molecular abundances observed towards TMC-1 with predictions from gas-grain models at 10 K.

	Observation	Model P1 (3×10^6 yr)	Model P2 (10^7 yr)
H_2O	<7.0(−8)[1]	2.8(−8)	4.0(−8)
O_2	<3.2(−6)[2]	1.4(−7)	4.2(−8)
CO	8.0(−5)[3]	1.5(−5)	1.3(−5)
NH_3	2.0(−8)[4]	4.3(−8)	1.2(−7)
HC_3N	6.0(−8)[4]	1.5(−9)	4.8(−9)

Note: $a(-b)$ implies $a \times 10^{-b}$
Refs.: [1] Snell et al. (2000b), [2] Goldsmith et al. (2000), [3] Ohishi et al. (1992), [4] Ohishi & Kaifu (1998).

better agreement than P1 at late times because gas-phase abundances are generally higher (see Fig. 1). Although cosmic ray desorption undoubtedly results in a C/O gas-phase elemental abundance ratio that increases with time, the effect does not reproduce the late-time results in Fig. 3.

The bottom panel of Fig. 4 compares the H_2O and O_2 abundances from the models with the upper limits set by SWAS, and also compares the modelled and observed CO abundances. Interestingly, the predicted amount of O_2 is almost always below the limit observed by SWAS. However, the low H_2O limit is only reproduced for times ≥ 2–3×10^6 yr, at which time the CO abundance is at least 2–3 times lower than is observed, and decreases monotonically with increasing time. At a time of 1×10^7 yr, where model P2 shows a secondary peak for overall agreement with observation, the predicted CO abundance is ∼6 times too low. This level of agreement is probably acceptable given observational uncertainties, although the deviation becomes greater for still later times.

In Table 1, we compare observations with gas-grain model predictions for the five important species shown in Fig. 1 at the secondary times of best general agreement for models P1 and P2 (see Fig. 4). There is reasonable agreement for four of the species, including CO, but the predicted HC_3N abundance is more than 13 times lower than the observation. This poor agreement is not any better at early times; it derives from the recent order-of-magnitude increase in its estimated abundance based on hyperfine analysis (Ohishi & Kaifu 1998). We also note that the predicted H_2O abundances are only just below the SWAS upper limit; if this limit were to be revised downwards by any significant degree, we would require later times at which CO and HC_3N abundances would need to be even further depleted. Finally, the general agreement at these times is not as good as it is at the early-time peak in two senses: (1) fewer molecules are fit to within an order of magnitude, and (2) some molecules, such as most sulphur-bearing species, are off by several orders of magnitude.

If we vary the sticking coefficient of 0.5 used in the models, the level of best agreement for most species is still ∼80%, after 10^5 yrs, but the secondary peak in the percentage agreement becomes less pronounced the higher the value of the sticking coefficient. With a sticking coefficient of 0.1 the overall agreement reaches 60–70% after 10^7 yrs, but if the sticking coefficient is 1, the secondary peak, between 3×10^6 and 10^7 yrs, is only 45–55%, a range close to that of our standard models. Thus, with a sticking coefficient of 0.1, both models P1 and P2 are in reasonable agreement with the observations of TMC-1 at a time of 10^7 yrs. The H_2O and O_2 abundances lie below the SWAS upper limits, while the predicted CO and NH_3 abundances are within a factor of 2 of what is observed. The predicted HC_3N abundance, however, is still more than an order of magnitude too low.

In summary, our current gas-grain models do not optimally match all the observations of TMC-1 at one time, although a rather unphysical, low sticking coefficient results in better agreement than does our standard model. Considering that gas-phase models with C/O = 1 are able to match the observations fairly accurately at a single time, the discrepancy between observations and the standard gas-grain models may be due to deficiencies in these models, especially in the differential desorption rates. But, then again, the discrepancy may also be astronomical in origin. For example, different parts of TMC-1 may have different evolutionary times and the observations may not be sufficiently resolved to deconvolute contributions from cloud parts with differing ages.

There is some observational evidence that different parts of the TMC-1 cloud are indeed at different evolutionary stages. Several previous studies have noted the chemical differentiation between the "cyanopolyyne" (CP) and "ammonia" peaks (e.g. Olano et al. 1988; Pratap et al. 1997), which are separated by ∼0.32 pc, or 7.9 arcmin, only somewhat larger than the SWAS beam. Cyanopolyynes have their peak abundances towards the former, whereas emission from ammonia is brightest at the latter. A variety of explanations for this variation have been given (e.g. van Dishoeck et al. 1993; Bergin et al. 1996; Markwick et al. 2000), but perhaps the simplest, based on pure gas-phase models, is that the NH_3-peak is chemically more evolved than the CP-peak (Saito et al. 2002). To fully explain the SWAS results might require a convolution of predicted abundances throughout TMC-1 (Lee et al. 1996b).

3.2. L134N

If we now compare the results of our gas-grain models with ground-based observations of L134N (Fig. 5), we find that the early-time solution is no longer clearly preferred. This result is in agreement with pure gas-phase model calculations, in which a C/O elemental abundance of unity does not have the same effect as in TMC-1 (Terzieva & Herbst 1998). Instead, the time of best agreement for both models P1 and P2 is at 10^6 yr, although the peak percentage agreement is not as high as the early-time peak in TMC-1. A few predicted abundances at the time of peak agreement in L134N are listed in Table 2 for comparison with the observations.

As can be seen in Table 2, NH_3 and HC_3N abundances from both models are within a factor of 4 of the observations at 10^6 yr. The predicted H_2O abundance from model P2 is similar to the upper limit seen in L134N, but the O_2 abundance is almost twice as high, while in model P1 the H_2O abundance is ∼3 times lower than the upper limit and the O_2 abundance

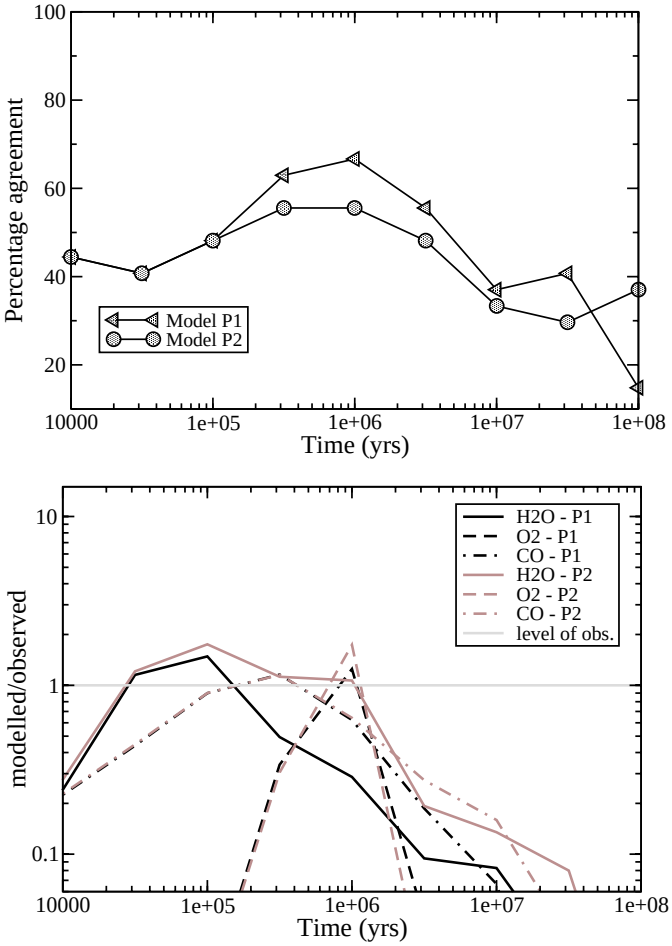

Fig. 5. Top: The percentage agreement of gas-grain chemical models (T = 10 K, $n(H_2) = 10^4$ cm^{-3}) with the 27 species observed by Ohishi et al. (1992) and Dickens et al. (2000). Bottom: The ratios of the predicted abundances of H_2O, O_2 and CO to the limits set/observations made towards L134N.

Table 2. A comparison of molecular abundances observed towards L134N with predictions from gas-grain models at 10 K.

	Observation	Model P1 (10^6 yr)	Model P2 (10^6 yr)
H_2O	<3.0(−7)[1]	8.6(−8)	3.2(−7)
O_2	<3.4(−6)[2]	4.2(−6)	5.9(−6)
CO	8.0(−5)[3]	5.0(−5)	5.1(−5)
NH_3	2.0(−7)[4]	6.1(−8)	7.3(−7)
HC_3N	2.0(−10)[4]	3.9(−10)	5.1(−10)

Note: $a(-b)$ implies $a \times 10^{-b}$
Refs.: [1] Snell et al. (2000b), [2] Goldsmith et al. (2000), [3] Ohishi et al. (1992), [4] Dickens et al. (2000).

is similar to the SWAS limit. These abundances are falling rapidly, so that after 2×10^6 yr the predicted amount of O_2 is ∼10 times lower than the SWAS limit, while H_2O is between 2.5 and 7 times lower, depending on the model.

Although the CO abundance is a few times lower than observed towards L134N by a time of 2×10^6 yr, it is in reasonable agreement, given the uncertainties inherent in obtaining accurate CO abundances observationally. We note, again, though, that if the upper limits on H_2O and O_2 abundance were more stringent, then matching the observations would require later times and, therefore, a lower CO abundance. In addition, the general agreement would be lower.

Table 3. A comparison of solid-state observations towards Elias 16 (Nummelin et al. 2001) with predictions from gas-grain models at 10 K.

	Observed	Model P1		Model P2	
		10^5 yr	10^6 yr	10^5 yr	10^6 yr
H_2O	$\sim 10^{-4}$	4.0(−5)	1.8(−4)	4.2(−5)	1.8(−4)
CO	26%	12.1	26.7	12.2	39.2
CO_2	23%	0.2	0.3	3.3(−3)	0.1
CH_3OH	<3.2%	1.5	2.8	2.0(−4)	9.5(−4)

Notes: $a(-b)$ implies $a \times 10^{-b}$; H_2O abundance is relative to H_2, the other ice abundances are listed as a percentage of H_2O.

3.3. Ice observations

Can the hypothesis that large portions of TMC-1 and L134N are at late times chemically be constrained by ice observations? One basic problem is that there is no suitable infrared continuum source behind either cloud core to allow absorption spectra of ice mantle components to be made. So, for the majority of ice components, one must consider the analogous source in front of the field star Elias 16, which lies behind the Taurus molecular cloud. The observed abundances or upper limits are listed in Table 3 for four species along with theoretical values at both early and late times, while theoretical values are plotted as a function of time in Fig. 6. What must be explained by theory are a large abundance of water ice, equal to much of the elemental oxygen abundance, amounts of CO and CO_2 ice equal to roughly 1/4 the water ice abundance, and a low upper limit for methanol ice.

In both models P1 and P2, the water ice abundance simply increases over time as oxygen atoms accrete onto the grains and are hydrogenated. To reach the observed level requires $\sim 10^6$ yr, although a significant fraction of this level is reached somewhat earlier in time. The observed abundance of CO ice is fit well by both models P1 and P2 at the late times listed in the table, but the predicted abundance is not significantly smaller at somewhat earlier times. We conclude that the comparison between theory and observation for these two ices gives some support to the late time hypothesis.

The O_2 ice abundance is not well determined, with only a high upper limit of 20% with respect to water ice, a limit set by Vandenbussche et al. (1999) towards NGC 7538 IRS9. Both models P1 and P2 show very low abundances of molecular oxygen ice, although the abundance of O_2-ice becomes much higher in model P2, where the diffusion of all species is slowed. This may seem counterintuitive, since slowing the diffusion of heavy species slows the rates of reaction between them. However, the majority of O_2 in model P2 comes from

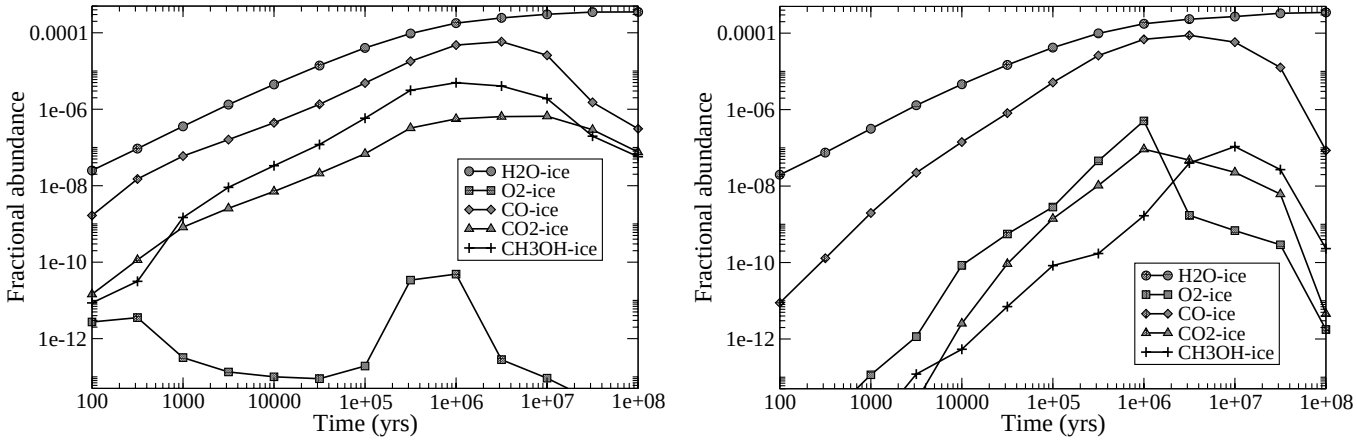

Fig. 6. Predicted abundances of grain surface species vs time, from models P1 (left) and P2 (right). $T = 10$ K; $n(H_2) = 10^4$ cm^{-3}.

accretion, and so is not greatly affected by any surface reactions. In model P1, it is the destruction of O_2 by O to make O_3, or by H in the series of reactions:

$$O_2 \xrightarrow{H} HO_2 \xrightarrow{H} H_2O_2 \xrightarrow{H} H_2O + OH, \quad (1)$$

making water ice, which keeps its surface abundance at 10^{-11} or less, with respect to H_2.

The abundance of methanol ice is low towards Elias 16, and this low abundance is easily reproduced by both models at all times. Note that CH_3OH ice has a much lower abundance in model P2 than P1, because it is produced by hydrogenation of CO on grain surfaces, a process which occurs much more slowly in model P2.

The only major problem with these models is the underproduction of CO_2. This was investigated and discussed in detail by Ruffle & Herbst (2001b), who found that, as long as diffusion rates are relatively rapid (model P1), a large CO_2-ice abundance can be obtained by a slight increase in either temperature (from 10 to 12 K) or H_2 density (from 10^4 to 10^6 cm^{-3}). The large CO_2 ice abundance can be achieved by 3×10^5 yr, however, so that CO_2 is not a good indicator of the age of the source.

Thus, in conclusion, ice abundances offer some evidence in favor of source ages equal to or in excess of 10^6 yr, although a source age of 3×10^5 yr or even somewhat younger is certainly not ruled out.

4. Star-forming regions

The temperatures of the star-forming regions observed by SWAS are ~20–50 K, and they have higher densities than the dark clouds, $\sim 10^5$ cm^{-3}. Gas-phase water was observed in these sources, with a fractional abundance significantly below the limits set in TMC-1 and L134N ($10^{-9} <$ [H_2O] < a few $\times 10^{-8}$; Bergin et al. 2000), while the upper limits on O_2 abundance are an order of magnitude lower than in cold clouds.

The gas-grain chemistry we are using is primarily designed to model dark clouds at 10 K, but, for completeness, we also compare SWAS observations with a few model runs at higher temperatures and densities. We note, however, that results for olivine are uncertain at temperatures significantly greater than 10 K, since the rate modifications may change with temperature (Ruffle & Herbst 2001b). Experimental evidence for H suggests that species on an amorphous carbon surface are more strongly bound (Katz et al. 1999), so that temperatures of ~20 K are required before the grain species are mobile enough for reactions to occur. The binding energies calculated for species on amorphous carbon are similar to those of a pure ice surface (Sandford & Allamandola 1988, 1991), so this model may be more appropriate if reactions occur on the surfaces of dust grains already coated in ice.

4.1. Chemistry on an olivine (silicate) surface

Figure 7 shows gas-phase abundances from models P1 and P2 with temperatures of 15 and 20 K, respectively, and H_2 densities of 10^5 cm^{-3}. The results for the two models are similar for the species shown. As was the case for dark clouds, the CO abundance rises for $\sim 10^5$ yr, peaking at $\sim 10^{-4}$ and then decreasing as CO freezes onto the grains. At these higher temperatures, however, there is a "plateau" between 3×10^5 yr and $\sim 4 \times 10^6$ yr where the CO abundance remains at $\sim 10^{-6}$ in model P1 and $\sim 3 \times 10^{-6}$ in model P2. This differs from the models at 10 K, where the CO abundance declines fairly steadily (Fig. 1), because CO desorbs from the grains more efficiently at the higher temperatures.

Figure 8 contains theoretical H_2O and CO abundances, relative to their observed abundances, and O_2 relative to the SWAS upper limit towards ρ Oph, one of the star-forming regions observed by SWAS that possesses a very low detected abundance of water. Again, the observed upper limit on the O_2 abundance does not present a problem, but, as the observed H_2O abundance towards this source is more than ten times lower than the limit set in the cold clouds, it now becomes a more serious problem for the models to reproduce the water observation without predicting a heavy depletion of CO.

The problem is further quantified in Table 4. The models do not predict a heavy depletion of NH_3, so its abundance is in good agreement with observations at all times $<10^8$ yr. However, for times between 10^6 and 10^7 yr, when the predicted H_2O abundance has fallen to ~twice the SWAS value,

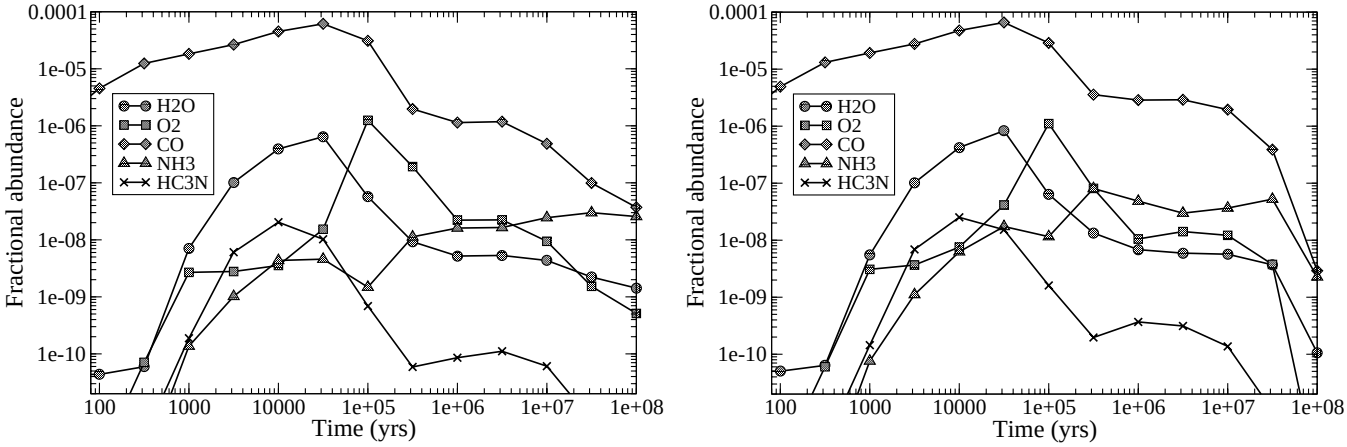

Fig. 7. Predicted gas-phase molecular abundances vs time, from models P1, $T = 15$ K (left) and P2, $T = 20$ K (right); $n(H_2) = 10^5$ cm^{-3}.

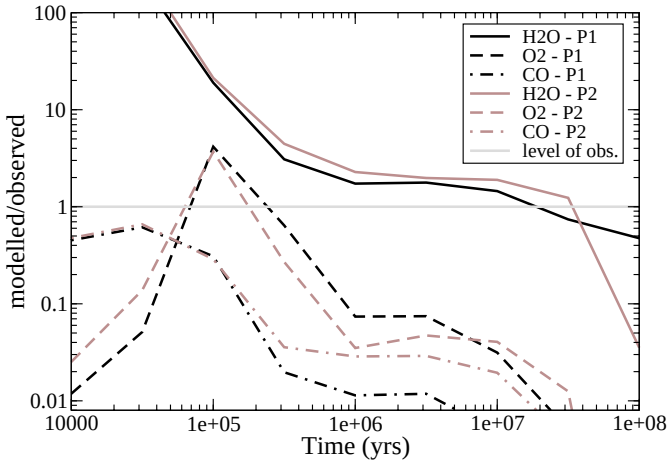

Fig. 8. The ratios of the predicted abundances of H_2O, O_2 and CO to the limits set/observations made towards ρ Oph. Model P1 uses $T = 15$ K, model P2 uses $T = 20$ K; $n(H_2) = 10^5$ cm^{-3}.

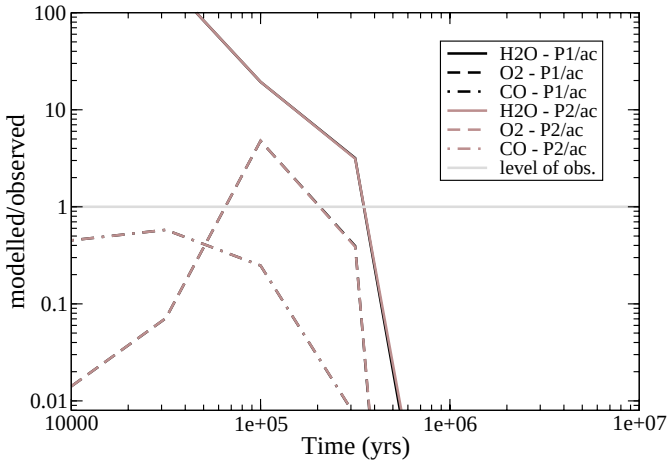

Fig. 9. The ratios of the predicted abundances of H_2O, O_2 and CO to the limits set/observations made towards ρ Oph. Models use $T = 20$ K, $n(H_2) = 10^5$ cm^{-3}. The results are nearly identical for the two models so only three distinct lines are seen.

Table 4. A comparison of molecular abundances observed towards ρ Oph with predictions from gas-grain models.

	Observed	Model P1		Model P2	
T (K)		15	15	20	20
(yr)		10^6	3×10^7	10^6	3×10^7
H_2O	3.0(−9)[1]	5.2(−9)	2.2(−9)	6.8(−9)	3.7(−9)
O_2	<3.(−7)[2]	2.2(−8)	1.5(−9)	1.1(−8)	3.8(−9)
CO	∼1.(−4)[3]	1.1(−6)	9.9(−8)	2.9(−6)	3.9(−7)
NH_3	3–10(−8)[4]	1.6(−8)	3.0(−8)	4.8(−8)	5.2(−8)

Note: $a(-b)$ implies $a \times 10^{-b}$
Refs.: [1] Snell et al. (2000a), [2] Goldsmith et al. (2000), [3] Myers et al. (1978), [4] Mizuno et al. (1990).

the CO abundance is already almost two orders of magnitude lower than the observation. By the time the H_2O abundances from the model are in agreement with the observations, predicted CO abundances are $\sim 10^{-7}$. Even though the CO observation of Myers et al. (1978) may not be in the same direction or at the same resolution as the SWAS beam, the modelled CO abundance does not seem realistic for such an abundant and ubiquitous interstellar molecule.

We have looked at results from model P1 at 20 K, even though the surface rate coefficients are very uncertain at this higher temperature, in order to see whether this would cause more CO desorption and increase its abundance to the levels observed. This is not the case, though; instead the CO abundance declines even more rapidly because at the higher temperature it reacts on freeze-out to make CO_2. We also investigated increasing the elemental C/O ratio to 1, but found that, although there is a significant decrease in O_2 abundance at all times, the H_2O abundance is only reduced by a factor of 3 at its peak abundance, and that, at late times, the gas-phase H_2O abundance is similar to the standard model, with C/O = 0.4.

4.2. Chemistry on an amorphous carbon surface

Figure 9 contains a comparison of the theoretical abundances of H_2O, O_2 and CO from models P1/ac and P2/ac at 20 K with the observations of ρ Oph. For these species, abundances are

almost identical in models P1/ac and P2/ac. Once again, there is a discrepancy between the time required for depletion of water, and the fairly high CO abundance that is observed, but this time the gas-phase species freeze out very rapidly after a few $\times 10^5$ yr, because they are more tightly bound to grains and so can't desorb.

5. Discussion

In this paper, we have applied the results of gas-grain chemical models to the problem caused by the low abundances of gaseous O_2 and H_2O detected by SWAS in a variety of interstellar sources. In general, the models easily reproduce the O_2 result at almost all times, but reproduce the H_2O result only at late times, when a significant amount of the gas-phase water has accreted onto grain mantles. The molecular oxygen is reproduced at almost all times because its formation in the gas is rather slow and cannot keep up with accretion. Once water and oxygen freeze onto grains, they do not easily desorb at the temperatures considered here.

Our model includes surface reactions and desorption mechanisms for all species, and so is more "complete" than previous accretion models, such as those of Bergin et al. (2000) and Viti et al. (2001). However, our gas-grain model is at its weakest at late times since the gas-phase abundances are strongly affected by the uncertain desorption rates adopted. Depending on the source, the late-time hypothesis may or may not be in conflict with explanations for the abundances of other molecules. In the dark cloud L134N, our model is most successful in a general sense at a time of 1×10^6 yr, at which time the predicted abundances of water and oxygen are not greater than the SWAS upper limits. Towards the cyanopolyyne peak in the dark cloud TMC-1, our model is most successful in a general sense at early times, but reaches a second era of reasonable, if somewhat less successful agreement, at much later times. The upper limit to the water abundance can only be reproduced at the later times. Moreover, at these times, the predicted CO abundance is falling considerably if not dramatically below the observed value. The worst agreement between theory and observation occurs in denser, warmer regions such as the star-forming region towards ρ Oph observed by SWAS. Here, reproduction of the small water abundance at late times leads to a predicted abundance for CO that can be orders of magnitude below its observed value. Not all star-forming regions have water abundances as low as ρ Oph; its abundance in the extended Orion source is an order of magnitude higher, and so is less difficult to fit simultaneously with a high CO abundance.

It is useful to compare our results with selected other recent approaches directed at explaining the SWAS observations in dark clouds. Two such approaches are those of Viti et al. (2001) and Charnley et al. (2001).

Viti et al. (2001) have constructed many models with gas-phase chemistry and with accretion to study a variety of physical conditions. In some of their models, all heavy species remain on grains while in others, CO and N_2 are returned promptly to the gas following adsorption, while all other heavy species are not. In general, these authors conclude that for dark clouds, the SWAS results and selected other gas-phase abundances are accounted for by a late-time scenario, the duration of which depends on their assumptions. This conclusion is rather similar to ours. They have also run steady-state models under conditions which allow bistability; in this situation, the so-called "high ionization phase" explains the low abundance of molecular oxygen towards a variety of sites, but the low abundance of water is a problem.

Charnley et al. (2001) have tested a model of shock cycling, in which they follow post-shock gas which is accreting onto grains. Their results are similar to ours, in that they find reasonable agreement with the SWAS limits on H_2O in dark clouds, but fail to match the lower levels observed in other sources. Once again, a type of "late-time" solution is necessary.

It also should be mentioned that Spaans & van Dishoeck (2001), in their discussion of clumpiness as a source of low average water and oxygen abundances, state that time-dependent chemistry and freeze-out are important to explain the low abundances in dense quiescent objects. A major alternative explanation, that photodissociation can explain the low abundances of water and molecular oxygen (Casu et al. 2001), must be reconciled with the significant abundances of many other molecules.

Since gas-phase water is produced in our models via the dissociative recombination of H_3O^+, it is useful to see if a change in the uncertain branching fraction for the H_2O + H channel can improve the agreement with the SWAS observations (see also Viti et al. 2001). For the calculations reported in this paper, we have adopted the results of Neau et al. (2000), who found a branching fraction of 0.18 in storage ring experiments. This value is lower than the previous results of 0.33 (Vejby-Christensen et al. 1997) and 0.25 (Jensen et al. 2000), both from a second storage ring. However, Williams et al. (1996) measured a branching ratio for H_2O production of no more than 0.05. Use of this branching fraction, which is 3–4 times lower than adopted in our calculations, does make it somewhat easier to fit the SWAS data. In TMC-1, for example, the predicted water abundance at early time is now only a factor of 3 greater than the current upper limit, although it is not clear that this result is acceptable. For the star-forming region towards ρ Oph, the detected low water abundance and upper limit to the oxygen abundance can be fit at somewhat earlier times than heretofore considered (3×10^5 yr), but the predicted gas-phase CO abundance is still much too low at these times. Only at a time of $\approx 10^5$ yr, when the calculated values for water and oxygen are a factor of a few high, is the prediction for CO reasonable. We conclude that the lower branching fraction is useful but not a panacea.

If our hypothesis that the low abundance of gas-phase water is indeed the result of longer time scales than customarily considered is correct for all sources studied, then it is likely that the desorption of CO and other species in our gas-grain model is not handled adequately. More accurate determinations of the desorption rates, especially for CO, are needed; the CO rate is currently being investigated by both theoretical and experimental means (H. J. Fraser, private communication).

As the revised version of this paper was being submitted, we learned of the unpublished results from the Odin team that the upper limit to the gas-phase O_2 abundance in TMC-1 and L134N is approximately an order of magnitude lower than the

SWAS result, depending somewhat upon the spatial extent of the oxygen. From our results in Fig. 4 (TMC-1) and Fig. 5 (L134N), one can see that the new lower limit is met at late time for TMC-1 but requires a time of $\geq 2 \times 10^6$ yr for L134N. This latter time is somewhat longer than the optimum time of $1–2 \times 10^6$ yr discussed in our analysis.

Acknowledgements. The Astrochemistry Program at The Ohio State University is supported by The National Science Foundation (US). We thank the Ohio Supercomputer Center for time on their Cray SV1 machine.

References

Bergin, E. A., Snell, R. L., & Goldsmith, P. F. 1996, ApJ, 460, 343
Bergin, E. A., Melnick, G. J., Stauffer, J. R., et al. 2000, ApJ, 539, L129
Bettens, R. P. A., Lee, H.-H., & Herbst, E. 1995, ApJ, 443, 664
Caselli, P., Hasegawa, T. I., & Herbst, E. 1998, ApJ, 495, 309
Casu, S., Cecchi-Pestellini, C.-C., & Aiello, S. 2001, MNRAS, 325, 826
Charnley, S. B., Rodgers, S. D., & Ehrenfreund, P. 2001, A&A, 378, 1024
Dickens, J. E., Irvine, W. M., Snell, R. L., et al. 2000, ApJ, 542, 870
Fraser, H. J., Collings, M. P., McCoustra, M. R. S., & Williams, D. A. 2001, MNRAS, 327, 1165
Gerakines, P. A., Whittet, D. C. B., Ehrenfreund, P., et al. 1999, ApJ, 522, 537
Goldsmith, P. F., Melnick, G. J., Bergin, E. A., et al. 2000, ApJ, 539, L123
Goldsmith, P. F., Li, D., Melnick, G. J., et al. 2001, BAAS, electronic edition, 33(4), 149.06
Hartquist, T. W., Williams, D. A., & Viti, S. 2001, A&A, 369, 605
Hasegawa, T. I., & Herbst, E. 1993, MNRAS, 261, 83
Jensen, M. J., Bilodeau, R. C., Safvan, C. P., et al. 2000, ApJ, 543, 764
Katz, N., Furman, I., Biham, O., Pirronello, V., & Vidali, G. 1999, ApJ, 522, 305
Lee, H.-H., Bettens, R. P. A., & Herbst, E. 1996a, A&AS, 119, 111
Lee, H.-H., Herbst, E., Pineau des Forêts, G., Roueff, E., & Le Bourlot, J. 1996b, A&A, 311, 690
Markwick, A. J., Millar, T. J., & Charnley, S. B. 2000, ApJ, 535, 256
Melnick, G. J., Stauffer, J. R., Ashby, M. L. N., et al. 2000, ApJ, 539, L77
Millar, T. J., Farquhar, P. R. A., & Willacy, K. 1997, A&AS, 121, 139
Mizuno, A., Fukui, Y., Iwata, T., Nozawa, S., & Takano, T. 1990, ApJ, 356, 184
Myers, P. C., Ho, P. T. P., Schneps, H., et al. 1978, ApJ, 220, 864
Neau, A., Al Khalili, S., Rosén, S., et al. 2000, J. Chem. Phys., 113, 1762
Nummelin, A., Whittet, D. C .B., Gibb, E. L., Gerakines, P. A., & Chiar, J. E. 2001, ApJ, 558, 185
Ohishi, M., Irvine, W. M., & Kaifu, N. 1992, in Astrochemistry of Cosmic Phenomena, ed. P. D. Singh (Kluwer, Dordrecht), 171
Ohishi, M., & Kaifu, N. 1998, Faraday Discuss., 109, 205
Olano, C., Walmsley, C. M., & Wilson, T. L. 1988, A&A, 196, 194
Pratap, P., Dickens, J. E., Snell, R. L., et al. 1997, ApJ, 486, 862
Ruffle, D. P., Hartquist, T. W., Taylor, S. D., & Williams, D. A. 1997, MNRAS, 291, 235
Ruffle, D. P., & Herbst, E. 2000, MNRAS, 319, 837 (RHI)
Ruffle, D. P., & Herbst, E. 2001a, MNRAS, 322, 770 (RHII)
Ruffle, D. P., & Herbst, E. 2001b, MNRAS, 324, 1054
Saito, S., Aikawa, Y., Herbst, E., et al. 2002, ApJ, 569, 836
Sandford, S. A., & Allamandola, L. J. 1988, Icarus, 76, 201
Sandford, S. A., & Allamandola, L. J. 1991, Icarus, 87, 188
Shalabiea, O. M., Caselli, P., & Herbst, E. 1998, ApJ, 502, 652
Snell, R. L., Howe, J. E., Ashby, M. L. N., et al. 2000a, ApJ, 539, L93
Snell, R. L., Howe, J. E., Ashby, M. L. N., et al. 2000b, ApJ, 539, L101
Spaans, M., & van Dishoeck, E. F. 2001, ApJ, 548, L217
Terzieva, R., & Herbst, E. 1998, ApJ, 501, 207
Tielens, A. G. G. M., & Allamandola, L. J. 1987, in Interstellar Processes, ed. D. J. Hollenbach, & H. A. Thronson, Jr. (Dordrecht: Reidel), 397
Vandenbussche, B., Ehrenfreund, P., Boogert, A. C. A., et al. 1999, A&A, 346, L57
van Dishoeck, E. F., Blake, G. A., Draine, B. T., & Lunine, J. I. 1993, in Protostars and Planets III, ed. E. H. Levy, & J. I. Lunine (Tucson: Univ. Arizona Press), 163
Vejby-Christensen, L., Andersen, L. H., Heber, O., et al. 1997, ApJ, 458, 531
Viti, S., Roueff, E., Hartquist, T. W., Pineau des Forêts, G., & Williams, D. A. 2001, A&A, 370, 557
Williams, T. L., Adams, N. G., Babcock, L., Herd, C. R., & Geoghegan, M. 1996, MNRAS, 282, 413